

# A fast and robust method for simultaneous estimation of mean diffusivity and mean tensor kurtosis

Brian Hansen<sup>1</sup>, Torben E. Lund<sup>1</sup>, Ryan Sangill<sup>1</sup>, and Sune N. Jespersen<sup>1,2</sup>

<sup>1</sup>CFIN/MindLab, Aarhus University, Aarhus, Denmark, <sup>2</sup>Dept. of Physics and Astronomy, Aarhus University, Denmark

**Target audience:** Researchers with an interest in diffusion kurtosis imaging, diffusion-MR method development, and the clinical application of kurtosis imaging.

**Purpose:** Diffusion kurtosis imaging (DKI) is a popular extension of diffusion tensor imaging (DTI) accounting for nongaussian aspects of diffusion in biological tissue<sup>1</sup>. Recently, several studies have indicated enhanced sensitivity of mean kurtosis (MK) to tissue pathology, including stroke<sup>2,4</sup>. However, relatively lengthy acquisition time and postprocessing required to estimate kurtosis metrics hamper further investigations. Recently a fast acquisition and postprocessing scheme for estimation of mean tensor kurtosis was proposed and demonstrated on large diffusion MR data sets from fixed rat brain and in-vivo human brain<sup>5</sup>. This protocol requires only 13 diffusion weighted images (scan time less than one minute), followed by postprocessing of few seconds in duration. Here we consider a refinement with increased accuracy in the estimate of mean tensor kurtosis with minimal additional scan time and no added computational time.

**Theory:** The method in ref. 5 aims to estimate the orientational average  $\bar{W}$  of the kurtosis  $W(\hat{n}) = \sum_{ijkl} W_{ijkl} n_i n_j n_k n_l$  observed along a direction  $\hat{n}$ :  $\bar{W} = 1/(4\pi) \int d\hat{n} W(\hat{n}) = \text{Tr}(W)/5$ . Here  $W_{ijkl}$  is the kurtosis tensor<sup>1</sup> appearing in the cumulant expansion of the diffusion signal  $S$  (here normalized to  $b=0$ ):

$$\log S(b, \hat{n}) = -bD(\hat{n}) + (b^2/6)\bar{D}^2 W(\hat{n}) + O(b^4) \quad (1)$$

where  $D(\hat{n})$  is the diffusivity. Because of Eq. (1), linear combinations of  $W(\hat{n})$  along different directions as in the trace operation can be *directly estimated by combining log of signals with diffusion gradients along corresponding directions*. In ref. 5 a set of nine directions were proposed fulfilling

$$\frac{1}{15} \left( \sum_{i=1}^3 \log S(b, \hat{n}^{(i)}) + 2 \sum_{i=1}^3 \log S(b, \hat{n}^{(i+)}) + 2 \sum_{i=1}^3 \log S(b, \hat{n}^{(i-)}) \right) = -b\bar{D} + 1/6b^2 \bar{D}^2 \bar{W} \quad (2)$$

where  $\hat{n}^{(i)}$ ,  $\hat{n}^{(i+)}$  and  $\hat{n}^{(i-)}$  ( $i=1,2,3$ ), are defined as  $\hat{n}^{(1)} = (1,0,0)^T$ ,  $\hat{n}^{(1+)} = (0,1,1)^T$ ,  $\hat{n}^{(1-)} = (0,1,-1)^T$ , and similarly for  $i=2$  and  $3$ ; i.e., superscript  $i$  in  $\hat{n}^{(i+)}$  and  $\hat{n}^{(i-)}$  labels the position of the '0'. In order to extract  $\bar{W}$  using Eq. 2, an estimate of  $\bar{D}$  is required. This was previously<sup>5</sup> done by acquiring an additional 3 images along  $\hat{n}^{(i)} (x,y,z)$  at a b-value assumed low enough to neglect nongaussian diffusion, and estimating the mean apparent diffusivity from these 3 directions. This allows  $\bar{W}$  to be estimated from one b0 image (for normalization), three images at  $b_1$  (eg.  $\approx 1000$  s/mm<sup>2</sup>) and nine images at  $b_2$  (eg.  $\approx 2500$  s/mm<sup>2</sup>). As in ref. 5, we refer to this protocol as the 1-3-9 protocol, and the associated estimate of  $\bar{W}$  as  $\bar{W}_{139}$ . However, it has been shown that estimates of  $\bar{D}$  are improved by including the kurtosis term even at relatively low b-values<sup>6</sup>. Therefore, we consider an extension of the above strategy where signals from the nine directions listed above are acquired at two b-values,  $b_1$  and  $b_2$ . Thereby, we can form eq. 2 at two different b-values producing a system of two equations with two unknowns ( $\bar{D}$ ,  $\bar{W}$ ). Solving these, we obtain for  $\bar{W}$  and  $\bar{D}$ :

$$\bar{W} = 6b_1b_2(A_1b_2 - A_2b_1)/(b_1b_2^2 - A_2b_1^2)^2 \quad (3a) \quad \text{and} \quad \bar{D} = (b_1^2A_2 - b_2^2A_1)/(b_1b_2^2 - b_1^2b_2) \quad (3b)$$

where  $A_1$  and  $A_2$  denote the left hand side of eq. (2) for the first b-value ( $b_1$ ) and second b-value ( $b_2$ ) respectively. We refer to this protocol as the 1-9-9 protocol, and the associated estimate of  $\bar{W}$  as  $\bar{W}_{199}$ . An additional advantage of the new approach is the direct formula for  $\bar{W}$  (eq. (3a)), which allows e.g. its accuracy and precision to be explicitly computed as a function of diffusion weighting ( $b_1$ ,  $b_2$ ). Here we demonstrate this by analyzing the precision of the  $\bar{W}$  estimate in the human cortex for various choices of  $b_1$  and  $b_2$  assuming the diffusion signal to be Rician with SNR as in the experiments.

**Methods:** To evaluate the efficiency of the 1-9-9 scheme, we acquired ten data sets in a normal volunteer in one session. The data consisted of: a) two large data sets of 160 diffusion weighted images each ( $T$  protocol in<sup>8</sup>) and b) eight data sets using the 1-9-9 scheme. Each of the two large data sets (a) provided the full kurtosis tensor through a fit to eq. (1). Two ground truth maps of  $\bar{W}$  were then produced from the trace of the full kurtosis tensor. From each of the 1-9-9 data sets both  $\bar{W}_{139}$  and  $\bar{W}_{199}$  were obtained.

**Results:** As expected<sup>5</sup>,  $\bar{W}_{139}$  provides a good estimate of the true  $\bar{W}$  (fig. 1). We therefore focus on assessing the improvement in  $\bar{W}$  estimate obtained with the 1-9-9 scheme over the 1-3-9 scheme. On inspection, maps of  $\bar{W}_{139}$  and  $\bar{W}_{199}$  are both quite similar to maps of  $\bar{W}$  (fig. 1). A closer scrutiny reveals slight improvements in agreement between  $\bar{W}_{199}$  and  $\bar{W}$  over  $\bar{W}_{139}$ , e.g. as marked in fig. 1 with a black ellipse in the  $\bar{W}_{199}$  map. Generally, improved agreement is seen in areas of high  $\bar{W}$  which have extents found<sup>5</sup> to be underestimated in  $\bar{W}_{139}$  maps compared to the true  $\bar{W}$ .

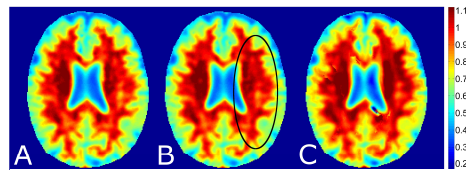


Fig. 1: A)  $\bar{W}_{139}$ ; B)  $\bar{W}_{199}$ ; C) 'True'  $\bar{W}$ .

Improved agreement outnumber the pixels where agreement went down. In fig. 3, we illustrate how the sum (over a large cortical ROI) of squared relative errors of  $\bar{W}$  depends on  $b_1$  and  $b_2$ . This map shows that slightly increased accuracy may be achievable using different values of  $b_1$  and  $b_2$ .

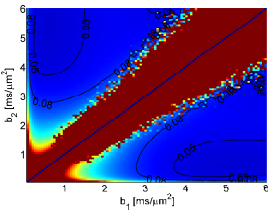


Fig. 3: map of sum of errors in  $\bar{W}$  estimate in the 1-9-9 scheme as function of b-values. Clearly,  $b_1$  and  $b_2$  should not be too close (red areas).

**Discussion and conclusion:** The 1-9-9 scheme has six additional measurements compared to the 1-3-9 scheme. This adds only a small amount of scan time, so even with the 1-9-9 scheme whole brain estimation of  $\bar{W}$  is possible in  $\sim 2$  min including postprocessing. The 1-9-9 strategy can naturally be extended to include more b-values (1-9-9-9...) allowing parameters to be calculated from an over-determined data set. This might increase parameter estimate accuracy in situations where the cost of longer scan time is acceptable. A possible further refinement to these strategies is inclusion of the inverted directions at each b-value to compensate for the effects of eddy currents. With almost 50% more data than 1-3-9, the 1-9-9 scheme gave a surprisingly small increase in accuracy. This is encouraging for

clinical use of the faster 1-3-9 scheme which has been shown<sup>5</sup> to provide an accurate estimate of  $\bar{W}$ . A clear advantage of the 1-9-9 scheme is that it allows explicit numerical optimization of the b-values used. Future study will show if the predicted improvement is experimentally discernible and whether optimized b-values from the 1-9-9 scheme can fruitfully be transferred to the faster 1-3-9 protocol.

**References:** 1. Jensen, J.H., et al., Magn. Reson. Med., (2005). 53:2. Hui, E.S., et al., Stroke, (2012); 3. Jensen, J.H., et al., NMR Biomed, (2011). 24:4. Latt, J., et al. in Proc. Int. Soc. Magn. Reson. Med. 2009; 5. Hansen et al. MRM 69(6) 2013; 6. Veraart et al. MRM 65, 2011; 8. Poot, D.H., et al., IEEE Trans Med Imaging, (2010). 29.

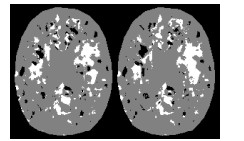


Fig. 2: White areas had improved  $\bar{W}$  estimate over eight trials of  $\bar{W}_{199}$  vs. eight trials of  $\bar{W}_{139}$ . Black areas had average reduction in accuracy. Gray pixels were neutral. Comparison vs. two maps of  $\bar{W}$  shown.